Second Quarterly Progress Report

NIH-NO1-DC-6-0002

Open Architecture Research Interface for Cochlear Implants

Philipos C. Loizou, Arthur Lobo, Nasser Kehtarnavaz, Venkat Peddigari, Hoi Lee, Murat Torlak, Lakshmish Ramanna, Serdar Ozyurt and Selami Ciftci

Department of Electrical Engineering
University of Texas-Dallas
2601 N. Floyd Rd
Richardson, TX 75080
Email: loizou@utdallas.edu

July 1, 2006 – September 30, 2006

1. Introduction

The main aim of this project is to develop a research interface platform which can be used by researchers interested in exploring new ideas to improve cochlear implant devices. This research platform includes a stimulator unit which can be used for electrical stimulation in animal studies, a recording unit for collecting evoked potentials from human subjects and a portable processor for implementing and evaluating novel speech processing algorithms after long-term use. The research platform chosen for this project is the personal digital assistant (PDA).

2. Summary of activities for the quarter

We continued with the development of speech coding algorithms on the PDA using LabVIEW. We also worked on recording EEG on the PDA, and continued with the design of a single-channel stimulator. We also started considering a wireless approach for transmitting signals from the PDA to the implant headpiece.

2.1 Real-time LabVIEW implementation of a 16-channel noise-band vocoder on the PDA

The thrust of our efforts during this quarter was placed on achieving real-time implementation of a 16-channel noise-band vocoder on the PDA platform. Considering that most algorithms in commercial implant devices are based on vocoders (Loizou, 2006), the implementation of a 16-channel noise-band vocoder was initially performed on the PC platform as reported in Loizou *et al.* (2006). Based on the LabVIEW PDA module, a graphical user interface (GUI) was designed as shown in Figure 1 to allow users to change the number of channels, filter type, filter order, filter cutoff frequency and observe their effect on the processing time and synthesized output.

Figure 1. Graphical interface for real-time LabVIEW implementation on the PDA.

To achieve real-time implementation of a 16-channel noiseband vocoder on the PDA, we used the real-time PC implementation as the starting point. Signal was acquired using the built-in microphone on a PDA device (HP X51). The processed frames were then passed through the noise-band vocoder software on the PDA to obtain synthesized frames which were played back to the PDA speaker as illustrated in Figure 2. The filter design stage was moved out of the real-time loop. Input frames of 100ms duration were acquired at a sampling rate of 22,050Hz. In general, in order to achieve a real-time throughput on the PDA platform, the total processing time for a frame should not exceed its frame length, which is 100ms in our case.

Several optimization steps were taken to achieve real-time throughput with the LabVIEW implementation. Table 1 shows the timing profiling outcome for the various steps taken. Using the profiling tools available in LabVIEW, we observed that the initial implementation, referred as Version A in Table 1, did not meet the real-time constraint as the total processing time for a 100ms frame was more than 1.8 seconds.

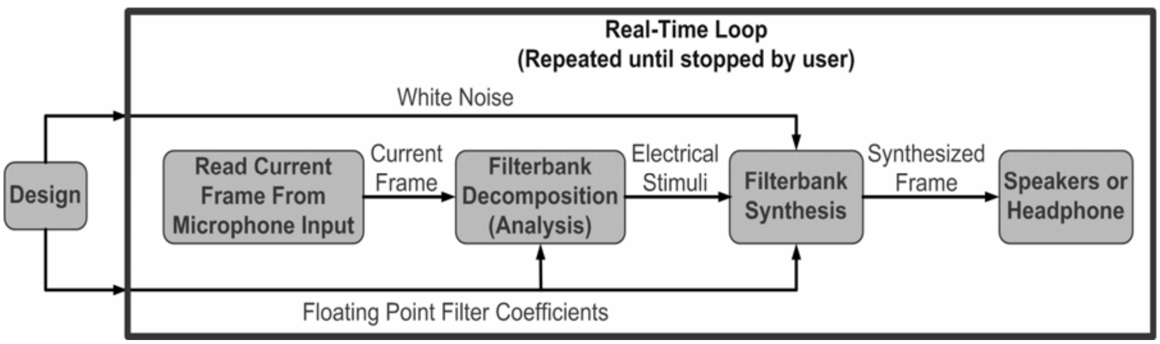

Figure 2. Real-time implementation (LabVIEW) process of a 16-channel noise-band vocoder on the PDA.

Sub-block or Component	**Processing time for 100ms length frames (ms)**			
	Version A	**Version B (A + DLL)**	**Version C (B + MA)**	**Version D (C + FPA)**
DC Offset Removal	7	5	3	1
Pre-Emphasis	11	8	5	3
Bandpass Filtering (Decomposition & Synthesis)	1450	705	412	34
Full-Wave Rectification	40	23	15	7
Lowpass Filtering	260	135	76	24
White-Noise Modulation	60	32	19	8
Total Processing Time	**1828**	**908**	**530**	**77**

Table 1. Timing outcome (msecs) corresponding to the various optimization steps taken that involved use of DLL libraries, memory allocation (MA) optimization and fixed-point arithmetic (FPA).

As shown in Table 1, the most time consuming components of the vocoder involved bandpass and low-pass filtering. To achieve a real-time throughput on the PDA platform, we took the following optimization steps: (a) use of Dynamic Link Libraries (DLL), (b) use of efficient Memory Allocation (MA) schemes and (c) use of Fixed-Point Arithmetic (FPA). Details for these optimization steps are provided in a submitted article (Pedigarri *et al.*, 2007). As shown in Table 1, Version D incorporated all the optimization steps which led to a processing time of 77ms for synthesizing speech frames corresponding to 100ms input signal frames. This version met the real-time constraint. It should be noted that in an actual cochlear implant device, only the filter decomposition (analysis) stage, which only requires 52ms, will be included.

The optimization steps (Pedigarri *et al.*, 2007) taken are general purpose in the sense that the same steps can be deployed to achieve real-time implementation of other clinical or industrial signal processing applications on PDAs. In our implementation, a hybrid programming approach (a combination of graphical and textual programming) was adopted (Kehtarnavaz *et al.*, 2007) where the Call Library Function node within the LabVIEW graphical programming environment is used to call C routines through DLLs.

2.2. EEG/EP data acquisition on the PDA

We began EEG/EP data acquisition on the PDA. As a first step, we started collecting EEG data using a basic amplifier setup. This setup included a single, differential amplifier (Grass model P511K) with an analog band-pass filter (1-100 Hz) that had a 12 dB/octave rolloff. This is a standard frequency range for recording the electroencephalogram (EEG) and for recording cortical auditory evoked potentials (CAEPs). The amplifier gain was set at x500. The active electrode was placed at the vertex location (CZ) of the subject's scalp, with a reference electrode placed on the right mastoid. The common/ground electrode was placed on the forehead. The electrodes were connected directly to the amplifier. The differential signal from the amplifier was sent to a compact flash data acquisition card (Dataq CF2, C-Cubed Ltd, UK), which sampled the incoming signal at 1000 Hz. Data was stored in PDA memory for later analysis. The Dataq-CF2 data acquisition card plugs into the compact flash slot of the PDA (see Figure 3). It has four 24-bit analog input lines, two 12-bit analog output lines and four digital I/O channels. It supports sampling rates up to 40 kHz.

The EEG/EP data acquisition set-up is shown in Figure 4.

Figure 3. Data acquisition card (Dataq CF2) used for recording EEG on PDA.

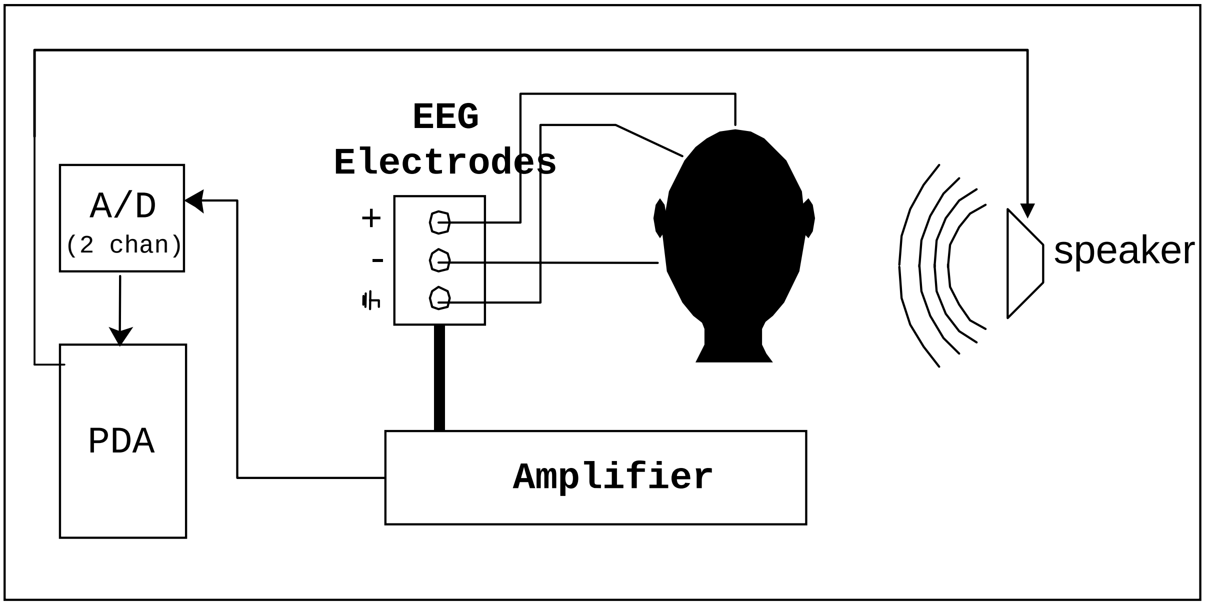

Figure 4. Schematic representation of the EEG/EP acquisition setup. The A/D block contains a Dataq-CF2 data acquisition card which plugs into the compact-flash (type 2) slot of the PDA. Only two of the four analog input lines of the A/D card were utilized for EEG recording.

At this point, we wanted to simply test the ability of the A/D card to sample a raw EEG signal on the PDA. We chose to record EEG at rest with eyes closed for a period of one minute. The purpose of this recording was to: 1) test the sampling capacity of the A/D card, 2) to verify portability of the stored data for further analysis, and 3) to analyze the sampled signal in the frequency domain in terms of typical EEG characteristics. Results of the EEG recording are shown in Figure 5. As seen in this figure, the one-minute EEG signal (shown with a 1 Hz high-pass filter to correct for DC drift) appears as random noise. This is an acceptable time-amplitude waveform for a raw EEG. However, the overall signal amplitude is a bit low, and this could be from an inadequate conversion of the amplifier gain to the dynamic range of the A/D card. Further testing will need to be performed in order to determine the correct conversion ratios for the stored voltage values.

In order to validate the EEG recordings, we imported the voltage values for each sample into the Scan 4.3 software (Compumedics/Neuroscan, El Paso, TX) for frequency analysis.

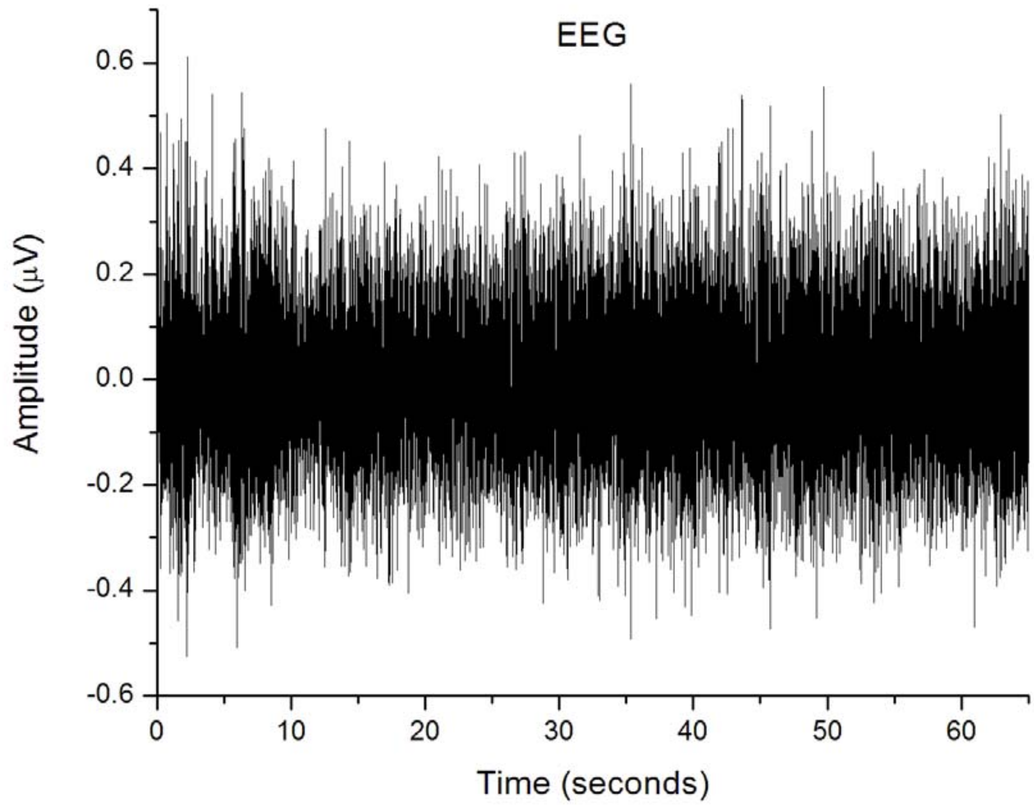

Figure 5. Time-amplitude waveform of EEG for a one-minute recording. EEG was acquired at rest with the eyes closed.

We performed two different frequency domain analyses on the raw EEG data. First, we performed an FFT on the one-minute EEG recording. This was done to test for activity that might be attributed to non-physiologic signals, as well as to ensure that physiologic activity appeared to contain standard low-frequency components. Figure 6 shows the long-term magnitude spectrum. As seen in this figure, most of the activity is between the 10 and 20 Hz frequency range. The 10-Hz activity, called Alpha activity, is the dominant activity in adults during a relaxed state (with eyes closed). The Alpha activity is typically accentuated over the posterior portion of the scalp. The 20-Hz activity, called Beta activity, is the dominant activity in adults during an active or anxious state. The Beta activity is typically accentuated over the frontal portion of the scalp. These results are reasonable in that during a short recording session (i.e., one minute) it is likely that the subject had some transition activity from Beta to Alpha. Furthermore, the vertex electrode used for the recording is roughly equidistant between the frontal and posterior positions that accentuate these two frequency bands. A large amount of noise is observed in the 70-100 Hz region. This is indicative of excess RF activity in the recording environment. This type of activity will likely be suppressed when using better quality amplifiers and when recording in a more ideal environment.

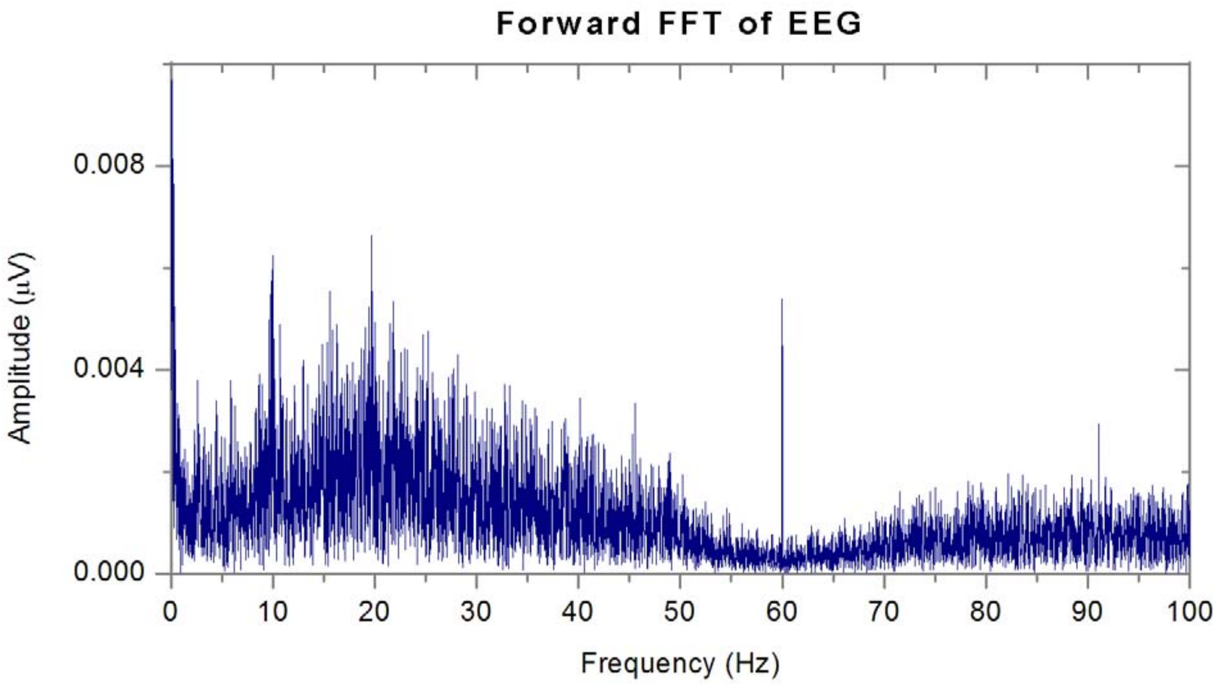

Figure 6. FFT magnitude spectrum obtained from a one-minute resting EEG waveforms. Figure shows information from peak activity at 10 (Alpha) and 20 Hz (Beta). Suppression of the activity around 60 Hz is seen as the result of a 60 Hz notch filter, implemented to reduce line-noise from the amplifier power supply.

The second frequency analysis examined the average magnitude spectrum of the EEG. This was accomplished by averaging the FFT magnitude spectra over 130 epochs of the raw EEG. This analysis provides us with information about the normal EEG frequency spectrum. For comparative purposes and as a reference, Figure 7 shows the frequency spectrum of a normal EEG (Malmivo & Plonsey, 1995). Figure 8 shows the average frequency spectrum for the resting EEG recorded on the PDA. Note the similarity in spectrum shape between Figures 7 and 8 (the frequency range is different in the two Figures). Some of the Delta activity (< 3 Hz) in Figure 8 is suppressed at the lower end probably due to the use of 1 Hz high-pass filter.

In summary, we successfully recorded a valid EEG signal on the PDA. Further tests are needed to examine EEG recordings with different settings of the amplifier. In the next quarter, we will focus on obtaining a CAEP response on the PDA.

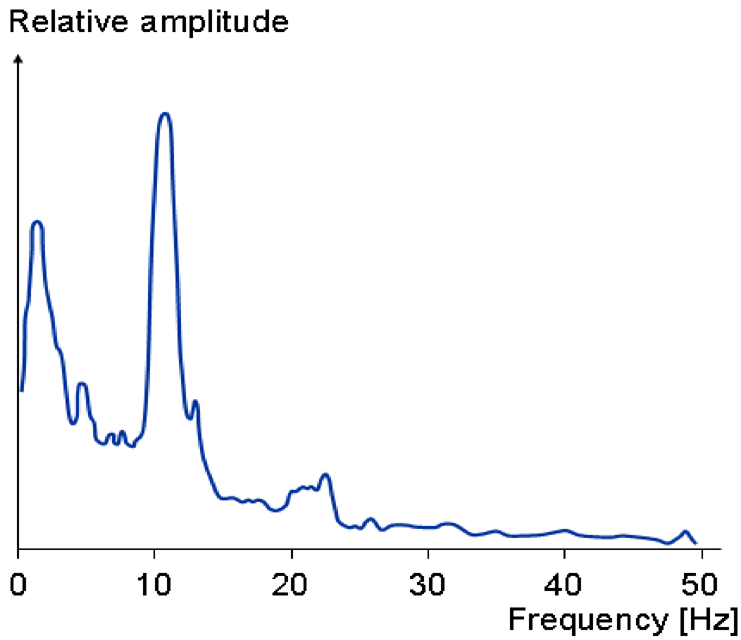

Figure 7. Frequency spectrum of a normal EEG (Malmivo & Plonsey, 1995).

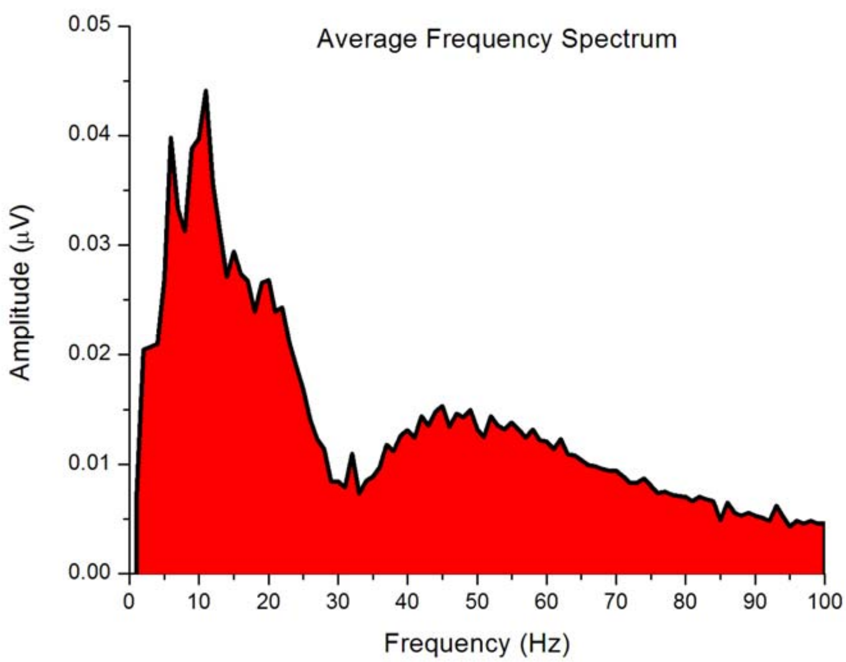

Figure 8. Average magnitude spectrum for resting EEG recorded on the PDA. This spectrum was computed by averaging the FFT spectra of 130 epochs of 512 samples from the continuous EEG waveform. The standard EEG signature is present with most of the energy in the 0-30 Hz range, and with peak activity in the Alpha band (7-13 Hz).

2.3 Design of single-channel stimulator

A new single-channel current stimulator has been designed to accommodate for a higher compliance voltage and a larger current amplitude range. The new single-channel stimulator incorporates a 9-bit resolution in stimulus current, and the current source is able to deliver current in the range of 2μA (lowest) to 1mA (highest). In addition, the input supply voltage of the current source is set to 5V to provide for a larger voltage compliance of 97%.

Figure 9 shows the structure of the new current source for the stimulation. The output capacitor interfaces between the electrode and the current source. The analog switch is used to define the direction of the current pulse in the active electrode with another reference stimulator. In the new single-channel stimulator, both binary-weighted current-source array and resistor switch arrays are employed to enhance the linearity of the current such that 9-bit resolution of the stimulus current can be achieved. C0-C8 and D0-D8 in Figure 9 are digital bits used to select the amount of current delivered to the electrode. Higher voltage compliance is achieved not only by using a higher input supply voltage of 5V but also by using a smaller voltage of Vb. In our design, when Vb is equal to 0.1V, the voltage compliance of 4.85V is obtained.

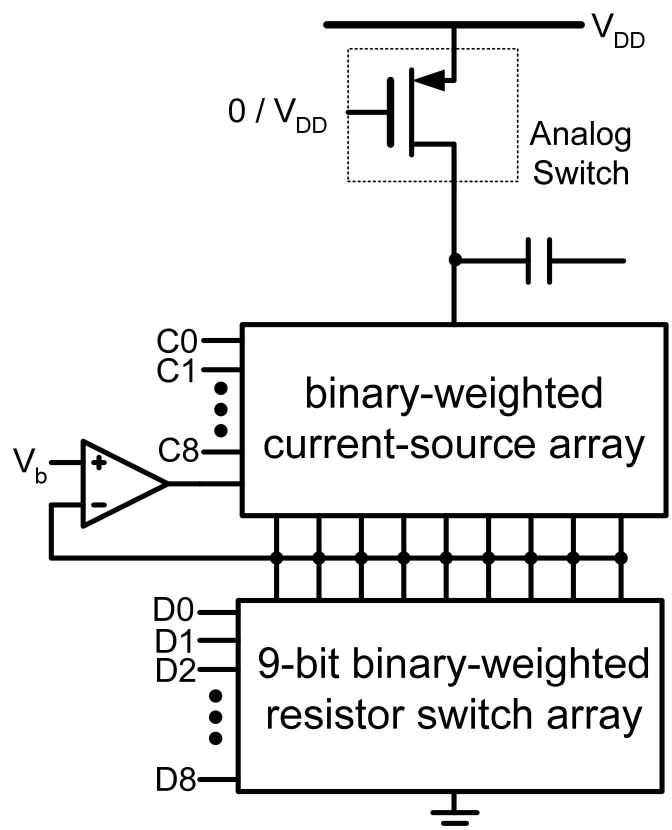

Figure 9. Block diagram of the new single-channel stimulator.

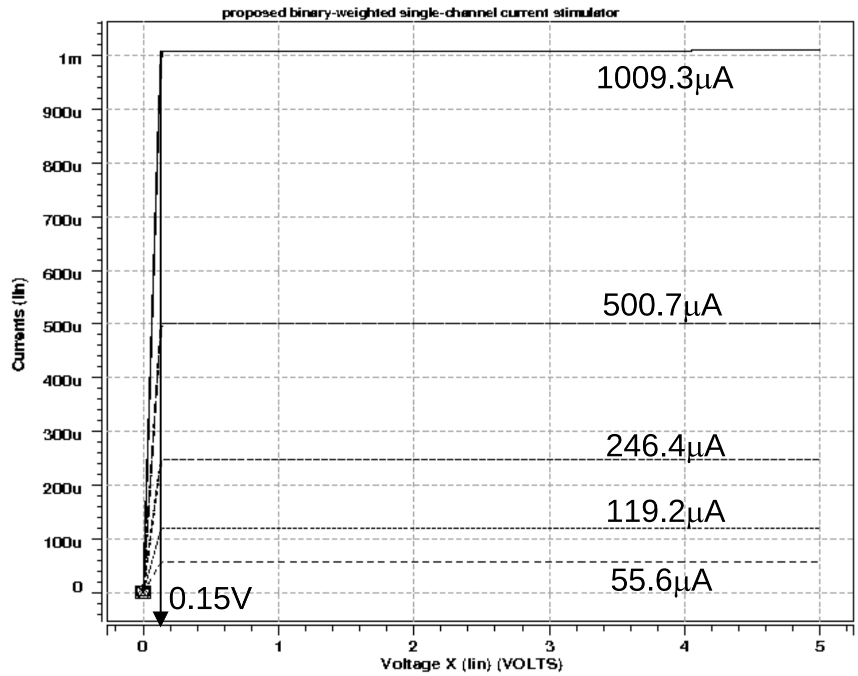

Figure 10. Simulation results of the stimulator system using the new current source.

Stimulation Amplitude (μA)	2-1000
Amplitude Digitization (bits)	9
Voltage Compliance	4.85V
Maximum Current Consumption (μA)	30
Supply Voltage	5V
Technology	AMS 0.35μm CMOS

Table 2 Simulation results of a single-channel current-controlled stimulator with new current source.

Figure 10 shows the Hspice simulation results of the single-channel stimulator. The figure plots the stimulus current (y-axis) versus different drain voltages of the current-source array used for modeling different electrode impedances (x-axis). A 9-bit resolution of the stimulus current is achieved ranging from 2μA to about 1mA. Figure 10 shows current step increments of 55.6μA, 119.2μA, 500.7μA and 1.009mA. The output stimulator achieves 97% voltage compliance from 0.15V to 5V, while constant stimulus current within 0.13% of the desired value is maintained under a 97% variation. Table 2 provides the summary of the simulation results.

2.4 Wireless implementation: First step

This project focuses on developing a PDA implant processor which is connected via a cable to the implant headpiece worn by the cochlear implant (CI) user. We started working, in parallel, on a wireless approach that would eliminate the cable connecting the implant headpiece to the PDA. In this approach, sound would be picked up by the microphone contained in the headpiece, and transmitted wirelessly to the PDA. The incoming sound would be processed by the PDA, and then transmitted wirelessly back to the implant headpiece (see Figure 11). This approach capitalizes on the fact most PDAs are already equipped with wireless technology (e.g., Wi-Fi, Bluetooth)). As a first possibility, we considered using Wi-Fi (Wireless Fidelity) since it is currently the most widely used wireless technology available in PDAs.

Wi-Fi refers to any type of wireless local area networks based on the IEEE 802.11b specification. Wi-Fi can be used for wireless LANS and provides 11 Mbps transmission (with a fallback to 5.5, 2 and 1 Mbps) in the 2.4 GHz band. Wi-Fi uses only Direct-Sequence Spread Sequence (DSSS) transmission technology. Many existing PDAs in the market come with integrated Wi-Fi support. We considered using Dell's Axim X51V PDA with Wi-Fi capability. The general structure of our proposed Wi-Fi implementation is shown in the Figure 11.

As a first step, we considered implementing a half-duplex speech transmission over wireless ad-hoc (peer-to-peer) networks between a PDA and a laptop running Windows XP. The source code for the PDA side was written using Microsoft Visual C++ 2005 integrated with Windows Mobile 5.0 SDK for Pocket PCs. We have utilized Microsoft P/Invoke library functions for the .NET Compact Framework. The code operates as follows. A TCP connection is first established between the two sides using socket programming techniques. The user speaks to the PDA's built-in microphone, and the speech signal is sampled, digitized and stored in memory. Then, the speech samples are directly transmitted wirelessly to the laptop side in ad-hoc mode. This process continues in a real-time playback mode until the user at the PDA side terminates audio transmission. In the next quarter, we will test and evaluate wireless transmission between two PDAs. Such a wireless configuration between two PDAs can potentially be used in assistive listening applications.

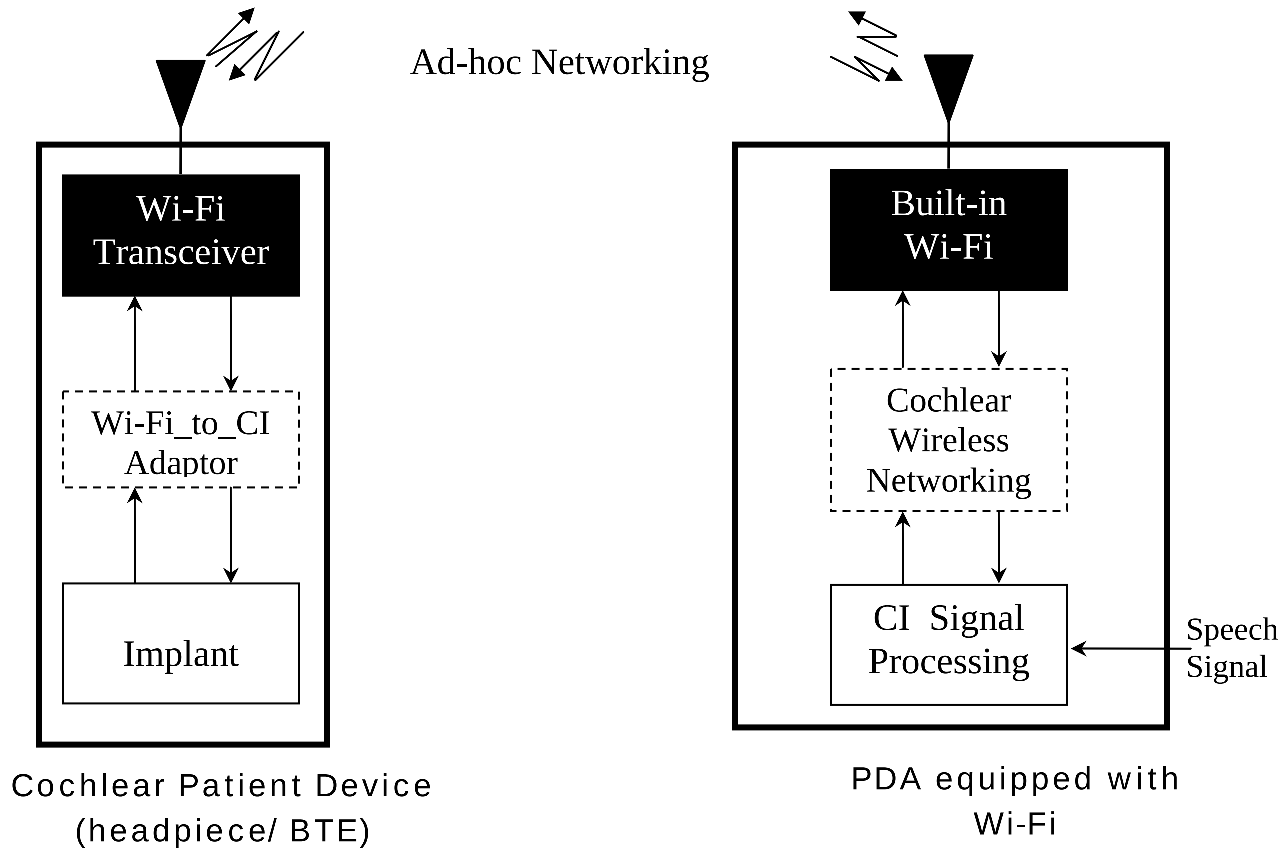

Figure 11. Conceptual diagram for the implementation of a wireless enabled cochlear implant processor based on Wi-Fi technology.

2.4 Other activities

- Presentation of an invited talk entitled "Noise reduction algorithms for cochlear implants and development of a PDA research interface" at Harvard University.
- Presentation of our plans and status of the present contract at "Neural Interfaces Workshop" sponsored and organized jointly by NINDS and NIDCD.

3. Plans for next quarter

- For the LabVIEW implementation of speech-coding algorithms, we will work on achieving real-time throughput for smaller (<100 ms) frame lengths. We will also address any accuracy issues rising due to the fixed-point arithmetic implementation.
- We will continue with our C implementation of the noise-band vocoder and profile the timing required by each signal-processing block.
- We will continue refining the design of the current stimulator (in terms of power optimization) and extend it to an 8-channel current stimulator, which can be fully integrated on a chip. In addition, we will also work on the hardware

implementation of the current stimulator for animal studies using discrete components.

- For the EEG/EP data acquisition on the PDA, we are planning the following activities:
  1) Make additional EEG recordings using different settings of the amplifier.
  2) Verification (using frequency analysis) of EEG recordings obtained from other amplifiers.
  3) Work on evoked potential (EP) data acquisition routines
- For the wireless implementation, we will test and assess the robustness of wireless transmission between two PDAs using Wi-Fi technology.

4. References

Kehtarnavaz, N., V. Peddigari, N. Kim, and Loizou, P. (2007). Hybrid programming for DSP lab courses: A cochlear implant system design project," submitted to *Proc. IEEE International Conference on Signal, Acoustics and Speech Processing.*

Loizou, P. (2006). "Speech processing in vocoder-centric cochlear implants," *Cochlear and Brainstem Implants* (ed. Moller, A.), Adv. Otorhinolaryngol. Basel, Karger, 64, 109–143.

Loizou, P., Lobo, A., Kehtarnavaz, N., Peddigari, V. and Lee, H. (2006). "Open architecture research interface for cochlear implants," *First Quarterly Progress Report*, NIH-NOI-DC-6-0002.

Malmivuo, J. and Plonsey, R. (1995). *Bioelectromagnetism: Principles and Applications of Bioelectric and Biomagnetic Fields.* Oxford University Press.

Peddigari, V., Kehtarnavaz, N. and Loizou, P. (2007). "Real-time LabVIEW implementation of cochlear implant signal processing on PDA platforms," submitted to *IEEE International Conference on Signal, Acoustics and Speech Processing*, 2007.

5. Appendix

Peddigari, V., Kehtarnavaz, N. and Loizou, P. (2006). "Real-time LabVIEW implementation of cochlear implant signal processing on PDA platforms," submitted to *IEEE International Conference on Signal, Acoustics and Speech Processing*, 2007.